

Dual unitarization scheme with several trajectories

M. Chaichian

Research Institute for Theoretical Physics, University of Helsinki, Finland

M. Hayashi

Department of Physics, Saitama College, Moroyama, Saitama, Japan

(Received 23 January 1978; revised manuscript received 21 April 1978)

Consequences of bootstrap with several input Regge trajectories are investigated. We find that in a general (without the duality-diagrams constraints) treatment of bootstrap, consistency requires the intercept of the output Pomeron pole in the one-dimensional case to be larger than one: $\alpha_P(0) > 1$, a situation reminiscent of the one in Reggeon field theory. Symmetry breakings of the Pomeron couplings are discussed. These couplings coincide with those of the f -dominated Pomeron model of Carlitz, Green, and Zee (CGZ). The case when in the unitarity loops all possible trajectories are exchanged is also considered. Predictions of the dual unitary model for the slopes of differential cross sections for diffractive scattering are made which differ from those of the CGZ model. A comparison with the experimentally available data is performed.

I. INTRODUCTION

Considerable interest has been devoted recently to a dual unitary program (dual unitarization) initiated originally by Veneziano¹ and Lee,² aiming at the construction of the topological Pomeron with the intercept $\alpha_P = 1$ and self-consistent Regge-pole generation in the absorptive part of 2→2-body scattering amplitudes, using unitarity and the quark-topology structure of the multi-Regge amplitudes. Many of the subsequent investigations along this line have proved that this program provides rather encouraging results, thus reproducing the basic features of high-energy scattering such as calculations of Pomeron effects, the Okubo-Zweig-Iizuka rule and its violation, and exotic exchanges, the breaking of exchange degeneracy both for meson and baryon trajectories.³ However, in the conventional dual unitary approach, one encounters with a certain difficulty the so-called f catastrophe⁴ which means that the f trajectory is not generated in the vacuum state since it is exactly canceled with the secondary Pomeron trajectory.

In the present paper we study the general case of the dual unitary model in which several input Regge trajectories are present. The treatment of several trajectories as input is a realistic case which is encountered in nature. We point out that a formal treatment of the model in a one-dimensional case (no t dependence) together with the imposed bootstrap on the output poles, generated out of three input Regge trajectories, yields a Pomeron with the intercept $\alpha_P > 1$. This result could be considered either as a certain difficulty of the model violating the Froissart bound or, alternatively, the >1 intercept could be attributed to the bare Pomeron—a situation reminiscent of the Reggeon field theory, where at superasymptotic energies

absorption is supposed to bring it down to unity. Also we show that one cannot generate Pomeron self-consistently out of two input Regge trajectories if one requires the intercept of the Pomeron α_P to be equal to 1. In other words, one again recovers $\alpha_P > 1$ also for the case of two input trajectories.

We have considered the case of several input trajectories by introducing sets of coupled integral equations and studying their Mellin transforms. With this technique we derive the SU_4 -broken couplings of the Pomeron to external particles (Reggeons) from where the ratios of different cross sections follow at high energies. We distinguish two different cases; the approximate case (a) and the exact case (b). In the approximate case (a), which could be called the "leading-trajectories approximation," we put in the loops of the unitarity sum only the (one) highest-lying Regge trajectory which is allowed by a duality diagram. In the exact case (b), we allow all the Regge trajectories which are permitted by duality diagrams to be exchanged in the unitarity sum.

We further derive the predictions of the dual unitary scheme for $2b(s)$, the slope of the differential cross section for the diffractive VN scattering defined as

$$b(s) = \frac{1}{2} (\partial / \partial t \ln d\sigma / dt)_{t=0}.$$

We discover that the predictions of the dual unitary model for these slopes are different from those of the f -dominated Pomeron of Carlitz, Green, and Zee (CGZ).⁵ We give these results and compare them with those derived by CGZ in the f -dominated model for the Pomeron. Comparison with the experimentally available data is performed.

In Sec. II we introduce the integral-equation technique as an illustration for the case of one Regge

trajectory and bootstrap both Regge and Pomeron sectors, recovering the known result $\alpha_P = 1$. We illustrate the disappearance of the f -trajectory (f catastrophe) and also derive the equal-spacing rules for Regge intercepts.

In Sec. III we consider the case of two and three input trajectories. We derive bootstrap equations for both Reggeon and Pomeron sectors and obtain the result of the Pomeron intercept being necessarily larger than one.

Section IV deals with a brief derivation of SU_4 -broken couplings of the Pomeron and its comparison with the f -dominated model of CGZ for the Pomeron⁶ which are further used in Sec. V.

Finally in Sec. V we derive the predictions of the model for the slope of the differential cross section for the diffractive scattering and they are distinct from those of the f -dominated Pomeron model.

II. DUAL UNITARY MODEL WITH ONLY ONE TRAJECTORY AS INPUT

A. The Reggeon sector

We take the dual unitary approach^{1,2} and use a multiperipheral production amplitude $A_{2 \rightarrow n}$ as an input to the unitarity equation

$$\text{Im} A_{2 \rightarrow 2} = \sum_n A_{2 \rightarrow n} A_{2 \rightarrow n}^* \quad (2.1)$$

One assumes that the production processes $2 \rightarrow n$ are described by the nondiffractive multi-Regge diagrams. Thus, the absorptive part for a multiperipheral (particle, cluster) production model is represented graphically as

$$\quad (2.2)$$

where b denotes the target and 1 denotes a particle on the Regge trajectory with intercept α_1 , the horizontal lines are narrow resonances (clusters), and a phase $e^{-i\pi\alpha}$ is associated with every exchanged (vertical) line.

In the input, planar (uncrossed) quark diagrams imply the exchanged objects (i.e., the vertical lines) to be exchange-degenerate Regge trajectories⁷ (ω - ρ - f - A_2 , K^* - K^{**} , ϕ - f' , etc.).

The unitarity equation (2.1) together with the summation of the multiperipheral ladders in (2.2) can be schematically written as the iterative solution of the integral equation

$$\quad (2.3)$$

where R denotes the amplitude with only uncrossed Regge exchanges, corresponding to the resonant part of the amplitude. The integral equation (2.3) simplifies if we perform the Mellin transform of the two-body scattering amplitude $A(s, t)$

$$A(j, t) = \int_0^\infty ds s^{-j-1} A(s, t),$$

and is reduced to the simple algebraic equation

$$A_{1b}^R(j) = \beta_{1b}^2 + g_{11}^2 \frac{1}{j - \alpha_{C1}} A_{1b}^R(j), \quad (2.4)$$

where β_{1b} and g_{11} denote the coupling constants of the corresponding vertex parts and

$$\alpha_{C1}(\bar{t}) = 2\alpha_1^{\text{in}}(\bar{t}) - 1. \quad (2.5)$$

We calculate the $2 \rightarrow 2$ forward amplitude ($t=0$) and take into account the t dependence of the input $2 \rightarrow n$ amplitudes by using \bar{t} as an effective value for all t after performing the phase-space integrals. The input Reggeon α_1^{in} in Eq. (2.5) is assumed to be the exchange-degenerate vector and tensor trajectory. The solution of (2.4) is

$$A_{1b}^R(j) = \frac{(j - \alpha_{C1}) \beta_{1b}^2}{j - (\alpha_{C1} + g_{11}^2)}. \quad (2.6)$$

The position of the output pole is determined as the zero of the denominator in (2.6) at

$$\alpha_R^{\text{out}}(t=0) = j = 2\alpha_R^{\text{in}}(\bar{t}) - 1 + g_{11}^2. \quad (2.7)$$

We assume further that \bar{t} is small and set it equal to zero (which is an exact statement for the one-dimensional case) everywhere:

$$\alpha_R^{\text{out}}(0) = 2\alpha_R^{\text{in}}(0) - 1 + g_{11}^2. \quad (2.8)$$

Requiring the bootstrap condition $\alpha_R^{\text{out}} = \alpha_R^{\text{in}} \equiv \alpha$, one obtains from Eq. (2.8)

$$\alpha = 1 - g_{11}^2. \quad (2.9)$$

Equation (2.9) implies $g_{11}^2 \simeq \frac{1}{2}$, if combined with the phenomenological value for the meson-trajectory intercept $\alpha_{\rho-f}(0) \simeq \frac{1}{2}$.

B. The Pomeron sector

The Pomeron is generated as the shadow of non-diffractive particle production processes. The topological Pomeron is the sum of all nonplanar duality diagrams in the s -channel unitarity sum which is expressed as the sum of all the diagrams in which each diagram has at least one twisted propagator.^{1,2} The integral equation for the Pomeron amplitude is represented in terms of dual unitary diagrams such as

$$\quad (2.10)$$

where the crosses on the propagator lines mean the twist of the diagram for which one has a Reggeon propagator $1 \times s^\alpha$ with the phase 1 (in contrast with the uncrossed propagator $e^{-i\pi\alpha} s^\alpha$ with the phase $e^{-i\pi\alpha}$). Here, because of the duality structure of the Pomeron, the inhomogeneous term [like the first term in the right-hand side of (2.3)] which would contribute only to the resonant part is absent. The integral equation (2.10) takes the following form, after transformation into angular momentum space:

$$\begin{aligned} A_P(j) &= g_{11} e^{-i\pi\alpha_1} \frac{1}{j - \alpha_{C1}} g_{11} e^{i\pi\alpha_1} A_P(j) \\ &+ g_{11} \frac{1}{j - \alpha_{C1}} g_{11} A_P(j) + g_{11} \frac{1}{j - \alpha_{C1}} g_{11} A_R(j) \\ &= 2g_{11}^2 \frac{1}{j - \alpha_{C1}} A_P(j) + g_{11}^2 \frac{1}{j - \alpha_{C1}} A_R(j). \end{aligned} \quad (2.11)$$

Since the phases for untwisted ($e^{-i\pi\alpha} e^{i\pi\alpha} = 1$) and for twisted ($1 \times 1 = 1$) are equal, the two first graphs in (2.10) are equal and therefore give the factor 2 in Eq. (2.11). The solution of (2.11) for $A_P(j)$, after the use of (2.6), is

$$A_P(j) = \frac{g_{11}^2 \beta_{1b}^2 (j - \alpha_{C1})}{(j - \alpha_{C1} - 2g_{11}^2)(j - \alpha_{C1} - g_{11}^2)}. \quad (2.12)$$

The leading singularity is at

$$(\alpha_P^{\text{out}})_1 = j = 2\alpha_R^{\text{in}} - 1 + 2g_{11}^2. \quad (2.13)$$

There is also a nonleading singularity at

$$(\alpha_P^{\text{out}})_2 = 2\alpha_R^{\text{in}} - 1 + g_{11}^2. \quad (2.14)$$

However, it exactly cancels the topological f meson, since at the singularity point given by (2.14), from Eq. (2.12) one has the residue

$$\frac{g_{11}^2 \beta_{1b}^2 (j - \alpha_{C1})}{j - \alpha_{C1} - 2g_{11}^2} = -g_{11}^2 \beta_{1b}^2, \quad (2.15)$$

which is equal but with an opposite sign to the residue of Eq. (2.6) given by $(j - \alpha_{C1}) \beta_{1b}^2 = g_{11}^2 \beta_{1b}^2$ at the position of the f -meson pole (2.8), i.e., at $\alpha_f^{\text{out}} = 2\alpha_R^{\text{in}} - 1 + g_{11}^2$. So, from Eqs. (2.6) and (2.12), one has for the total scattering amplitude (with the vacuum number in the t channel)

$$A = \text{P} + \text{f} = \frac{(j - \alpha_{C1}) \beta_{1b}^2}{j - \alpha_{C1} - 2g_{11}^2}. \quad (2.16)$$

One sees that the amplitude (2.16) has only the Pomeron pole given by (2.13). Therefore, in the total amplitude (sum of Pomeron and Reggeon contributions), only the leading Pomeron survives and the f trajectory is canceled with the nonleading

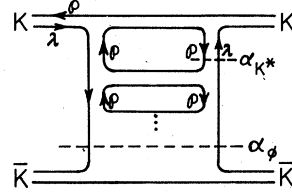


FIG. 1. Diagrammatic derivation of Eq. (2.19).

Pomeron singularity,⁸ thus causing the so-called “ f catastrophe”⁴ (see, however, Ref. 5).

Equations (2.8) and (2.13), after the elimination of g_{11}^2 , give the known results of Lee² and Veneziano,¹

$$\alpha_P^{\text{out}} = 2(\alpha_R^{\text{out}} - \alpha_R^{\text{in}}) + 1, \quad (2.17)$$

which gives

$$\alpha_P^{\text{out}} = 1 \quad (2.18)$$

when the bootstrap condition $\alpha_R^{\text{out}} = \alpha_R^{\text{in}}$ is imposed on the output and input Regge poles.

Equation (2.8) has interesting consequences for the intercepts of the Regge trajectories. For instance, from $K\bar{K}$ scattering, which is shown diagrammatically in Fig. 1, one gets

$$\alpha_\phi = 2\alpha_{K^*} - 1 + g^2, \quad (2.19)$$

where the internal λ quark in the loops has been neglected. Equations (2.19) and (2.9) give the equal-spacing rule for the intercepts (α_i denotes everywhere the intercept)

$$\alpha_\phi + \alpha_\rho = 2\alpha_{K^*}, \quad (2.20)$$

which, in the case of linearly rising Regge trajectories, gives the known quark mass formula.

Similarly, considering the $D\bar{D}$ scattering (Fig. 2), one gets

$$\alpha_\psi = 2\alpha_{D^*} - 1 + g^2, \quad (2.21)$$

where again the internal λ and c quarks in the loops (Fig. 2) have been neglected. Equations (2.21) and (2.9) give the relation

$$\alpha_\psi + \alpha_\rho = 2\alpha_{D^*}. \quad (2.22)$$

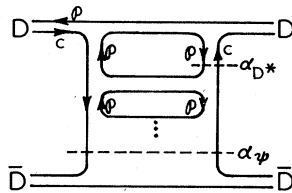


FIG. 2. Diagrammatic derivation of Eq. (2.21).

III. TWO AND THREE INPUT TRAJECTORIES

A. Dual bootstrap with two input trajectories

Reggeon sector. Here we develop the formalism which was illustrated for the case of one trajectory in the previous section, and generate output poles from two input Regge trajectories (say, π and ρ). The closed set of unitarity integral equations in this case is presented as follows:

$$(3.1)$$

where 1 and 2 denote the particles on the Regge trajectories with intercepts α_1 and α_2 .⁹ In the Mellin transform space from (3.1) one obtains

$$A_{1b}^R(j) = \beta_{1b}^2 + g_{11}^2 \frac{1}{j - \alpha_{C1}} A_{1b}^R(j) + g_{12}^2 \frac{1}{j - \alpha_{C2}} A_{2b}^R(j), \quad (3.2)$$

$$A_{2b}^R(j) = \beta_{2b}^2 + g_{21}^2 \frac{1}{j - \alpha_{C1}} A_{1b}^R(j) + g_{22}^2 \frac{1}{j - \alpha_{C2}} A_{2b}^R(j),$$

where $\alpha_{Ci} = 2\alpha_i^{\text{in}} - 1$ ($i = 1, 2$), α_i^{in} is the intercept of input trajectory, and all the other notations are as in Sec. II.

The positions of the output poles are determined from the vanishing of the determinant of (3.2), i.e.,

$$j^2 - (\alpha_{C1} + \gamma_{11} + \alpha_{C2} + \gamma_{22})j + (\alpha_{C1} + \gamma_{11})(\alpha_{C2} + \gamma_{22}) - \gamma_{12}^2 = 0, \quad (3.3)$$

where $\gamma_{ij} \equiv g_{ij}^2$.

Pomeron sector. The Pomeron sector can be treated analogously. The dual unitary equations are graphically presented as

$$(3.4)$$

In the Mellin-transform space one has for (3.4)

$$\begin{aligned} \left(1 - \frac{2\gamma_{11}}{j - \alpha_{C1}}\right) A_1^P(j) - \frac{2\gamma_{12}}{j - \alpha_{C2}} A_2^P(j) \\ = \frac{\gamma_{11}}{j - \alpha_{C1}} A_1^R(j) + \frac{\gamma_{12}}{j - \alpha_{C2}} A_2^R(j), \\ - \frac{2\gamma_{12}}{j - \alpha_{C1}} A_1^P(j) + \left(1 - \frac{2\gamma_{22}}{j - \alpha_{C2}}\right) A_2^P(j) \\ = \frac{\gamma_{12}}{j - \alpha_{C1}} A_1^R(j) + \frac{\gamma_{22}}{j - \alpha_{C2}} A_2^R(j). \end{aligned} \quad (3.5)$$

The output poles for the Pomeron amplitudes A_i^P are determined from an equation analogous to Eq. (3.3), in which γ_{ij} is replaced by $2\gamma_{ij}$, i.e., from

$$j^2 - (\alpha_{C1} + 2\gamma_{11} + \alpha_{C2} + 2\gamma_{22})j + (\alpha_{C1} + 2\gamma_{11})(\alpha_{C2} + 2\gamma_{22}) - 4\gamma_{12}^2 = 0. \quad (3.6)$$

However, actually one cannot formulate bootstrap out of two (e.g., π and ρ) Reggeons self-consistently, unless the intercept of the Pomeron trajectory is greater than one. We show this, using the relations between the input and output trajectories in the Reggeon and Pomeron sectors and also the bootstrap condition. Equation (3.3) has two solutions, α_1^{out} and α_2^{out} , which satisfy

$$\alpha_1^{\text{out}} + \alpha_2^{\text{out}} = \alpha_{C1} + \alpha_{C2} + \gamma_{11} + \gamma_{22}, \quad (3.7)$$

$$\alpha_1^{\text{out}} \alpha_2^{\text{out}} = (\alpha_{C1} + \gamma_{11})(\alpha_{C2} + \gamma_{22}) - \gamma_{12}^2. \quad (3.8)$$

Equation (3.6) has two solutions, α_1^P and α_2^P [$\alpha_i^P \equiv (\alpha_i^{\text{out}})^{\text{out}}$], which satisfy

$$\alpha_1^P + \alpha_2^P = \alpha_{C1} + \alpha_{C2} + 2\gamma_{11} + 2\gamma_{22}, \quad (3.9)$$

$$\alpha_1^P \alpha_2^P = (\alpha_{C1} + 2\gamma_{11})(\alpha_{C2} + 2\gamma_{22}) - 4\gamma_{12}^2, \quad (3.10)$$

From Eqs. (3.7) and (3.9) one has

$$\alpha_1^P + \alpha_2^P = 2(\alpha_1^{\text{out}} - \alpha_1^{\text{in}}) + 2(\alpha_2^{\text{out}} - \alpha_2^{\text{in}}) + 2. \quad (3.11)$$

Equation (3.11) is the generalization of the relation (2.17). Imposing the bootstrap condition¹⁰ $\alpha_1^{\text{out}} = \alpha_1^{\text{in}}$ and $\alpha_2^{\text{out}} = \alpha_2^{\text{in}}$ one obtains from (3.11)

$$\alpha_1^P + \alpha_2^P = 2. \quad (3.12)$$

If one demands for one of the Pomerons $\alpha_1^P = 1$, then one has

$$\alpha_1^P = \alpha_2^P = 1. \quad (3.13)$$

It follows from (3.13) together with the use of Eqs. (3.9) and (3.10) and the inequality

$$(\alpha_{C1} + 2\gamma_{11} + \alpha_{C2} + 2\gamma_{22})^2 \geq 4(\alpha_{C1} + 2\gamma_{11}) \times (\alpha_{C2} + 2\gamma_{22}) \quad (3.14)$$

that $\gamma_{12}^2 \leq 0$. One concludes, therefore, that either

$$\gamma_{12}^2 = 0 \quad (3.15)$$

or the intercept of the leading output Pomeron pole is larger than one:

$$\alpha_P(0) > 1. \quad (3.16)$$

The decoupling result (3.15) contradicts the general idea of bootstrap out of two trajectories through the coupled channels, while the conclusion (3.16) could be regarded either as a certain difficulty of the model violating the Froissart bound or, alternatively, the intercept > 1 could be attributed to the bare Pomeron—a conclusion reminiscent of the situation in the Reggeon field theory,¹¹ where, at

ultra-asymptotic energies, absorption is supposed to bring it down to one. In fact, as discussed frequently in recent literature,¹² a Pomeron with an intercept >1 can even have several appealing phenomenological features.¹³

We note that in this case as well, one encounters the f catastrophe: For a total amplitude which is the sum of Pomeron and f Reggeon $A_i = A_i^P + A_i^R$ ($i=1, 2$), one obtains, by summing up Eqs. (3.2) and (3.5), the following system of equations:

$$\begin{aligned} \left(1 - \frac{2\gamma_{11}}{j - \alpha_{C1}}\right) A_1 - \frac{2\gamma_{12}}{j - \alpha_{C2}} A_2 &= \beta_{1b}^2, \\ -\frac{2\gamma_{12}}{j - \alpha_{C1}} A_1 + \left(1 - \frac{2\gamma_{22}}{j - \alpha_{C2}}\right) A_2 &= \beta_{2b}^2. \end{aligned} \quad (3.17)$$

The equation which determines the output singularities of (3.17) coincides with Eq. (3.6). However, note that Eq. (3.6) gives only the leading Pomeron singularities, while the solution of Eq. (3.5) contains the Reggeon singularities (with the f -quantum number) as well, in the same way as for the case of one input trajectory where they appeared previously in Eq. (2.12). But now, in the total amplitudes given by (3.17), only the two Pomeron singularities survive, whose positions are given by (3.6), and whose nonleading poles have exactly canceled the corresponding f trajectories of the Reggeon section.

B. Dual bootstrap with three input trajectories

Reggeon sector. The system of s -channel unitarity integral equations for the case of three input Regge trajectories, denoted by 1, 2, and 3, is presented in the Mellin transform space as

$$A_i^R(j) = \beta_i^2 + \sum_{i'=1,2,3} \frac{\gamma_{ii'}}{j - \alpha_{Ci'}} A_{i'}^R(j) \quad (i=1, 2, 3). \quad (3.18)$$

The positions of the output Reggeon are obtained from the vanishing of the determinant of (3.18),

$$j^3 - Aj^2 + Bj - C = 0, \quad (3.19)$$

where

$$\begin{aligned} A &= x_1 + x_2 + x_3, \\ B &= x_1 x_2 + x_2 x_3 + x_3 x_1 - (\gamma_{12}^2 + \gamma_{23}^2 + \gamma_{31}^2), \\ C &= x_1 x_2 x_3 - \gamma_{23}^2 x_1 - \gamma_{31}^2 x_2 - \gamma_{12}^2 x_3 + 2\gamma_{12} \gamma_{23} \gamma_{31}, \end{aligned} \quad (3.20)$$

with $x_1 = \alpha_{C1} + \gamma_{11}$, $x_2 = \alpha_{C2} + \gamma_{22}$, and $x_3 = \alpha_{C3} + \gamma_{33}$. The condition [that the two extrema of (4.4) have opposite signs] under which Eq. (3.19) has three real roots α_i^{out} ($i=1, 2, 3$) is

$$C^2 + \frac{2}{27}A(2A^2 - 9B) \leq \frac{1}{27}B^2(A^2 - 4B). \quad (3.21)$$

By allowing the couplings γ_{ij} to be in a certain domain, one can assume that the condition (3.21) is indeed fulfilled.

Pomeron sector. The Pomeron bootstrap can be treated along the same lines as in Sec. IIIA. The positions of the output poles are determined from an equation similar to that of the Reggeon sector (3.19) in which everywhere γ_{ij} is replaced by $2\gamma_{ij}$, i.e., from

$$j^3 - A'j^2 + B'j - C' = 0, \quad (3.22)$$

where

$$\begin{aligned} A' &= x'_1 + x'_2 + x'_3, \\ B' &= x'_1 x'_2 + x'_2 x'_3 + x'_3 x'_1 - 4(\gamma_{12}^2 + \gamma_{23}^2 + \gamma_{31}^2), \\ C' &= x'_1 x'_2 x'_3 - 4\gamma_{23}^2 x'_1 - 4\gamma_{31}^2 x'_2 \\ &\quad - 4\gamma_{12}^2 x'_3 + 16\gamma_{12} \gamma_{23} \gamma_{31}, \end{aligned} \quad (3.23)$$

with $x'_1 = \alpha_{C1} + 2\gamma_{11}$, $x'_2 = \alpha_{C2} + 2\gamma_{22}$, and $x'_3 = \alpha_{C3} + 2\gamma_{33}$. Similar to inequality (3.21), the condition for (3.22) having three real roots $(\alpha_i^P)^{\text{out}}$ ($i=1, 2, 3$) is expressed as

$$C'^2 + \frac{2}{27}A'(2A'^2 - 9B') \leq \frac{1}{27}B'^2(A'^2 - 4B'). \quad (3.24)$$

Under the assumption of the validity of (3.21) and (3.24), the singularity positions of output Reggeons and Pomerons can be obtained from Eqs. (3.19) and (3.22), respectively. However, similar to the case of bootstrap with two input trajectories, a formal bootstrap with three input (say π , ρ , and ϵ) Reggeons in a one-dimensional model yields necessarily a Pomeron with intercept larger than one, $\alpha_P(0) > 1$. We illustrate this point in the following way: One has from Eqs. (3.19) and (3.22)

$$\sum_{i=1}^3 \alpha_i^{\text{out}} = \sum_{i=1}^3 (\alpha_{Ci} + \gamma_{ii}), \quad (3.25)$$

$$\sum_{i=1}^3 (\alpha_i^P)^{\text{out}} = \sum_{i=1}^3 (\alpha_{Ci} + 2\gamma_{ii}). \quad (3.26)$$

It follows that

$$\sum_{i=1}^3 (\alpha_i^P)^{\text{out}} = 2 \sum_{i=1}^3 (\alpha_i^{\text{out}} - \alpha_i^{\text{in}}) + 3. \quad (3.27)$$

Note that this is the generalization of the results (2.17) and (3.11) for the one- and two-trajectory cases. Imposing the bootstrap condition

$$\alpha_i^{\text{out}} = \alpha_i^{\text{in}} \quad (i=1, 2, 3), \quad (3.28)$$

one obtains from (3.27)

$$(\alpha_1^P)^{\text{out}} + (\alpha_2^P)^{\text{out}} + (\alpha_3^P)^{\text{out}} = 3. \quad (3.29)$$

Of course, in order to check the self-consistency of the whole scheme, one has to check the self-consistency of the bootstrap condition (3.28) in the Reggeon sector separately (also see Ref. 10).

Analogous to the two-trajectory case, the possibility

$$(\alpha_1^P)^{\text{out}} = (\alpha_2^P)^{\text{out}} = (\alpha_3^P)^{\text{out}} = 1, \quad (3.30)$$

which satisfies (3.29), is ruled out from the following considerations: If (3.30) is the case, then one has

$$A' = x'_1 + x'_2 + x'_3 = 3, \quad (3.31)$$

$$B' = x'_1 x'_2 + x'_2 x'_3 + x'_3 x'_1 - 4(\gamma_{12}^2 + \gamma_{23}^2 + \gamma_{31}^2) = 3, \quad (3.32)$$

$$C' = x'_1 x'_2 x'_3 - 4\gamma_{23}^2 x'_1 - 4\gamma_{31}^2 x'_2 - 4\gamma_{12}^2 x'_3 - 16\gamma_{12}\gamma_{23}\gamma_{31} = 1. \quad (3.33)$$

Eliminating x'_3 from Eqs. (3.31) and (3.32), one obtains

$$x_1'^2 + (x_2' - 3)x_1' + x_2'^2 - 3x_2' + 4(\gamma_{12}^2 + \gamma_{23}^2 + \gamma_{31}^2) + 3 = 0. \quad (3.34)$$

However, this equation does not have real roots for x_1' (and also for x_2'), while

$$x_1' = \alpha_{C1} + 2\gamma_{11} = 2\alpha_1^{\text{in}} - 1 + 2g_{11}^2$$

must be real since both the input trajectory α_1^{in} and the coupling constant g_{11}^2 are real. Therefore, one is led to the conclusion that the case (3.30) is ruled out and one recovers the result

$$\alpha_P(0) > 1, \quad (3.35)$$

which may have some bearing upon the situation in Reggeon field theory¹¹ and can even have several phenomenologically appealing properties¹² as were already mentioned.

We have considered the case with target b fixed [see (3.18)]. Considerations of different targets do not change our conclusions, since by adding some of the equations, the primary system of equations can be brought to a set equivalent to the case with the target fixed. Further, in deriving (3.35), we have been allowing the coupling constants $\gamma_{ij} \cong g_{ij}^2$ to have any value, since our derivations were independent of values γ_{ij} in the equations. However, this result has been obtained in a one-dimensional (no t dependence) dual unitary model. Whether the above-mentioned result could be altered in a model with the realistic dimension by the proper inclusion of the t dependences is not known, due to the fact that in this case one cannot treat the problem analytically. Let us also mention that in the case of three input trajectories, the f trajectories cancel out with the nonleading parts of the Pomeron amplitudes in the same manner as discussed previously for the one- and two-trajectory cases.

IV. SU_4 -BROKEN POMERON COUPLINGS IN DUAL UNITARY SCHEME AND COMPARISON WITH THE f -DOMINATED POMERON MODEL OF CGZ⁶

In this and the next sections we study questions of more practical interest and apply the formalism developed in the previous section to obtain the

Pomeron couplings⁴ to external particles, while in the next section we find the predictions of the dual unitary model for the slopes of the differential cross sections for various vector-meson-nucleon diffractive scatterings. We assume that SU_4 is broken for the Regge trajectories according to

$$\alpha_1 > \alpha_2 > \alpha_3 > \alpha_4 > \alpha_5 > \alpha_6, \quad (4.1)$$

where α_i denotes the intercept of the Regge trajectory i with the notation

$$1 = \rho, \quad 2 = K^*, \quad 3 = \phi, \quad 4 = D^*, \quad 5 = F^*, \quad 6 = \psi. \quad (4.2)$$

For the moment, we do not impose the symmetry (SU_4) requirements on the coupling constants $\gamma_{ij} = g_{ij}^2$ and leave them arbitrary. We distinguish two different cases: (a) *the leading-trajectory approximation*, in which we put in the loops of the unitarity sum only the (one) highest-lying [according to (4.1)] Regge trajectory which is allowed by duality diagram and *the exact case (b)*, where we allow all the Regge trajectories, which are permitted by duality diagrams, to be exchanged in the unitarity sum.

Case (a). To begin, as an illustration, we consider ϕN scattering. For the absorptive part of ϕN -diffractive scattering, the dual unitary equation is presented:

$$\text{Diagram} = \text{Diagram}_1 + \text{Diagram}_2. \quad (4.3)$$

The graphical notation in (4.3) is obvious—although we are dealing with amplitudes, but since the Pomeron is a factorized pole in the dual unitary model, we no longer draw the target but only the Pomeron (wavy) line; also in (4.3) we have dropped, on the right-hand sides, the diagrams which contain Regge amplitudes.

Clearly, one has to consider the twisted external particles as well,

$$\text{untwisted} \equiv \text{twisted}$$

where external quark lines are ordered clockwise, while in the twisted diagrams, the quark enters in the reversed order.

Let us call the untwisted external particle amplitude A and the twisted one B . Then in the Mellin transform space Eq. (4.3) reads as

$$A_3^P = \frac{\gamma_{23}}{j - \alpha_{C2}} (A_2^P + B_2^P). \quad (4.4)$$

Since the physical particle has both orientations of

quarks, it is composed of twisted and untwisted lines and so the physical amplitude \bar{A}_i is expressed as $\bar{A}_i^P = \frac{1}{2}(A_i^P + B_i^P)$. For ρ , ϕ , and ψ one has $\bar{A}_i^P = A_i^P$ ($i=1, 3, 6$), since $A_i = B_i$ for $i=1, 3, 6$. Thus (4.4) gives

$$\bar{A}_3^P = \frac{2\gamma_{23}}{j - \alpha_{C2}} \bar{A}_2^P. \quad (4.5)$$

We impose the bootstrap condition on the output Pomeron $j^{\text{out}} = \alpha_P(0)$. Multiplying Eq. (4.5) by $(j - \alpha_P(0))$ and taking $\lim_{j \rightarrow \alpha_P(0)}$, one obtains

$$\beta_3^P = \frac{\gamma_{23}}{\alpha_P - \alpha_2} \beta_2^P, \quad (4.6)$$

where

$$\bar{\alpha}_P = \frac{1 + \alpha_P(0)}{2} \quad (4.7)$$

and the Pomeron residues β_i^P are defined as $\alpha_i^P = \lim_{j \rightarrow \alpha_P(0)} (j - \alpha_P(0)) \bar{A}_i^P$. One can proceed for other external particles in a similar way. Then for amplitudes \bar{A}_i^P and residues β_i^P we obtain the following: For K^*N scattering

$$\bar{A}_2^P = \frac{\gamma_{22}}{j - \alpha_{C2}} \bar{A}_2^P + \frac{\gamma_{21}}{j - \alpha_{C1}} \bar{A}_1^P \quad (4.8)$$

and

$$\beta_2^P = \frac{(\bar{\alpha}_P - \alpha_2)\gamma_{21}/2}{(\bar{\alpha}_P - \alpha_1)(\bar{\alpha}_P - \alpha_1 - \gamma_{11}/2)} \beta_1^P;$$

for D^*N scattering

$$\bar{A}_4^P = \frac{\gamma_{41}}{j - \alpha_{C1}} \bar{A}_1^P + \frac{\gamma_{44}}{j - \alpha_{C4}} \bar{A}_4^P \quad (4.9)$$

and

$$\beta_4^P = \frac{(\bar{\alpha}_P - \alpha_4)\gamma_{41}/2}{(\bar{\alpha}_P - \alpha_1)(\bar{\alpha}_P - \alpha_4 - \gamma_{44}/2)} \beta_1^P;$$

for F^*N scattering

$$\bar{A}_5^P = \frac{\gamma_{52}}{j - \alpha_{C2}} \bar{A}_2^P + \frac{\gamma_{54}}{j - \alpha_{C4}} \bar{A}_4^P \quad (4.10)$$

and

$$\beta_5^P = \frac{1}{4} \frac{1}{\bar{\alpha}_P - \alpha_1} \left(\frac{\gamma_{52}\gamma_{21}}{\bar{\alpha}_P - \alpha_2 - \gamma_{22}/2} + \frac{\gamma_{54}\gamma_{41}}{\bar{\alpha}_P - \alpha_4 - \gamma_{44}/2} \right) \beta_1^P;$$

for ψN scattering

$$\bar{A}_6^P = \frac{2\gamma_{64}}{j - \alpha_{C4}} \bar{A}_4^P \quad (4.11)$$

and

$$\beta_6^P = \frac{\gamma_{64}\gamma_{41}/2}{(\bar{\alpha}_P - \alpha_1)(\bar{\alpha}_P - \alpha_4 - \gamma_{44}/2)} \beta_1^P;$$

and for ρN scattering

$$\bar{A}_1^P = \frac{2\gamma_{11}}{j - \alpha_{C1}} \bar{A}_1^P \quad (4.12)$$

and

$$\beta_1^P = \frac{\gamma_{11}}{\alpha_P - \alpha_1} \beta_1^P.$$

Note that Eq. (4.12) implies the relation which coincides with (2.19). Equations (4.6)–(4.11) give the ratios of Pomeron couplings β_i^P , and hence the total-cross-sections ratios. If all coupling constants g_{ij}^2 preserve SU_4 symmetry, i.e., all possible quark diagrams have equal weight irrespective of whether they contain \mathcal{O} , λ , or c quarks, then

$$\gamma_{ij} = g_{ij}^2 = g^2. \quad (4.13)$$

Thus (4.12) can be written as $g^2 = \gamma_{ij} = \bar{\alpha}_P - \alpha_1$, and from (4.6)–(4.11) one gets

$$R_2 \equiv \frac{\sigma(K^*N)}{\sigma(\rho N)} = \beta_2^P/\beta_1^P = \frac{1}{2}[1 + r_1(0)], \quad (4.14)$$

$$R_3 \equiv \frac{\sigma(\phi N)}{\sigma(\rho N)} = \beta_3^P/\beta_1^P = r_1(0), \quad (4.15)$$

$$R_4 \equiv \frac{\sigma(D^*N)}{\sigma(\rho N)} = \beta_4^P/\beta_1^P = \frac{1}{2}[1 + r_2(0)], \quad (4.16)$$

$$R_5 \equiv \frac{\sigma(F^*N)}{\sigma(\rho N)} = \beta_5^P/\beta_1^P = \frac{1}{2}(R_3 + R_6), \quad (4.17)$$

$$R_6 \equiv \frac{\sigma(\psi N)}{\sigma(\rho N)} = \beta_6^P/\beta_1^P = r_2(0), \quad (4.18)$$

where

$$r_1(0) = \frac{\bar{\alpha}_P(0) - \alpha_1(0)}{\bar{\alpha}_P(0) - \alpha_3(0)}, \quad (4.19)$$

$$r_2(0) = \frac{\bar{\alpha}_P(0) - \alpha_1(0)}{\bar{\alpha}_P(0) - \alpha_6(0)}.$$

From Eqs. (4.14)–(4.18) one obtains the known quark-model relations

$$2\sigma(K^*N) = \sigma(\rho N) + \sigma(\phi N),$$

$$2\sigma(D^*N) = \sigma(\rho N) + \sigma(\psi N), \quad (4.20)$$

$$2\sigma(F^*N) = \sigma(\phi N) + \sigma(\psi N).$$

Under exchange degeneracy $\alpha_V(0) = \alpha_T(0)$ [see paragraph after Eq. (2.2)], i.e., $\alpha_\rho = \alpha_f$ and $\alpha_P(0) = 1$, which implies $\bar{\alpha}_P(0) = \alpha_P(0)$, the relations (4.14)–(4.18) coincide⁴ with those obtained in the framework of the f -dominated Pomeron^{6,14} model of Carlitz, Green, and Zee,⁶ in which one has

$$r_1^{\text{CGZ}}(0) = \frac{\alpha_P(0) - \alpha_f(0)}{\alpha_P(0) - \alpha_{f'}(0)}, \quad (4.21)$$

$$r_2^{\text{CGZ}}(0) = \frac{\alpha_P(0) - \alpha_f(0)}{\alpha_P(0) - \alpha_{f_c}(0)}.$$

It is necessary, however, to emphasize the difference between the CGZ model and the dual unitarization scheme. In the f -dominated Pomeron model,⁶ one has f besides P , but the Pomeron behaves like an f coupling, while in the dual unitarity scheme, one has only the Pomeron singularity as discussed in Sec. II.

Broken SU_4 for the couplings. Symmetry breaking of the Pomeron couplings comes about through differences in the intercepts of the Regge trajectories even though all vertices satisfy exact SU_4 symmetry. One can introduce⁴ additional symmetry-breaking (suppression) factors $F_i F_j$ for the $q_i \bar{q}_j$ -meson production ($F_\phi = F_{31} = 1$) which would take into account symmetry breakings due to the masses of the produced particles,⁴ with different quark contents in the unitarity sum. Then the predictions of dual unitarization differ from those of the CGZ model.⁴ In this case, instead of (4.14)–(4.18) we have

$$R_2 = \frac{[1 + r_1(0)] F_\lambda}{2[1 + (1 - F_\lambda) r_1(0)]}, \quad R_3 = \frac{F_\lambda^3 r_1(0)}{1 + (1 - F_\lambda) r_1(0)},$$

$$R_4 = \frac{[1 + r_2(0)] F_C}{2[1 + (1 - F_C) r_2(0)]}, \quad R_5 = \frac{1}{2} \left(R_3 \frac{F_C}{F_\lambda} + R_6 \frac{F_\lambda}{F_C} \right),$$

$$R_6 = \frac{F_C^3 r_2(0)}{1 + (1 - F_C) r_2(0)}.$$

The simple quark-model relations (4.20) are not then satisfied. Assuming the following representative value for Pomeron and Reggeon intercepts:

$$\alpha_P(0) = 1, \quad \alpha_1 = \frac{1}{2}, \quad \alpha_2 = \frac{1}{4}, \quad \alpha_3 = 2\alpha_2 - \alpha_1 = 0,$$

$$\alpha_4 = (\alpha_1 + \alpha_6)/2 = \frac{1}{4} + \frac{1}{2}\alpha_6, \quad \alpha_5 = (\alpha_3 + \alpha_6)/2 = \frac{1}{2}\alpha_6,$$

and for the suppression factors $(F_\lambda, F_C) = (1, 1), (0.9, 0.8), (0.8, 0.7)$, we obtain the numerical values for $R_i = \sigma(V_i N)/\sigma(\rho N)$ for three different values of $\alpha_6(0) = -2, -4, -6$. They are summarized in Table I.

Case (b). If we calculate the Pomeron couplings by taking into account contributions from all possible trajectories in the loops of the unitarity sum, then for ϕN scattering, for instance, we have

$$\text{Diagram} = \sum_{i=2,3,5} \text{Diagram}_i + \text{Diagram}_i, \quad (4.22)$$

$$\bar{A}_3^P = \sum_{i=2,3,5} [2\gamma_{3i}/(j - \alpha_{ci})] \bar{A}_i^P.$$

Proceeding as in case (a) we obtain, with SU_4 -symmetric coupling constants, the following relations:

$$R_2 = \frac{1}{2}(R_3 + 1),$$

$$R_3 = \frac{-\frac{1}{2} \left(\frac{1}{g^2} - \frac{1}{\bar{\alpha}_P - \alpha_1} \right) + \frac{1 - (\bar{\alpha}_P - \alpha_5)/g^2}{2(\bar{\alpha}_P - \alpha_2)} + \frac{1}{2[1 - (\bar{\alpha}_P - \alpha_6)/g^2]} \left(\frac{1}{g^2} - \frac{1}{\bar{\alpha}_P - \alpha_1} - \frac{1}{\bar{\alpha}_P - \alpha_2} \right)}{\frac{1}{2(\bar{\alpha}_P - \alpha_3)} + \left(1 - \frac{\bar{\alpha}_P - \alpha_5}{g^2} \right) \left[\frac{1}{g^2} - \frac{1}{2(\bar{\alpha}_P - \alpha_2)} - \frac{1}{\bar{\alpha}_P - \alpha_3} \right] - \frac{1/g^2 - 1/(\bar{\alpha}_P - \alpha_2) - 1/(\bar{\alpha}_P - \alpha_3)}{2[1 - (\bar{\alpha}_P - \alpha_6)/g^2]}}$$

$$R_4 = (\bar{\alpha}_P - \alpha_4) \left[-\frac{R_3}{2(\bar{\alpha}_P - \alpha_2)} + \frac{1}{g^2} - \frac{1}{\bar{\alpha}_P - \alpha_1} - \frac{1}{2(\bar{\alpha}_P - \alpha_2)} \right], \quad (4.23)$$

$$R_5 = (\bar{\alpha}_P - \alpha_5) \left[\left(\frac{1}{g^2} - \frac{1}{2(\bar{\alpha}_P - \alpha_2)} - \frac{1}{\bar{\alpha}_P - \alpha_3} \right) R_3 - \frac{1}{2(\bar{\alpha}_P - \alpha_2)} \right],$$

$$R_6 = \frac{\bar{\alpha}_P - \alpha_6}{1 - (\bar{\alpha}_P - \alpha_6)/g^2} \left[-\left(\frac{1}{g^2} - \frac{1}{\bar{\alpha}_P - \alpha_2} - \frac{1}{\bar{\alpha}_P - \alpha_3} \right) R_3 + \frac{1}{\bar{\alpha}_P - \alpha_1} + \frac{1}{\bar{\alpha}_P - \alpha_2} - \frac{1}{g^2} \right].$$

Note that the above solutions are reduced to the relations (4.14)–(4.18) if the following two sets of relations are valid: (i) The relation which holds between the coupling constant g^2 and the Regge intercept

$$\frac{1}{g^2} = \frac{1}{\bar{\alpha}_P(0) - \alpha_1(0)} + \frac{1}{\bar{\alpha}_P(0) - \alpha_3(0)} + \frac{1}{\bar{\alpha}_P(0) - \alpha_6(0)}, \quad (4.24)$$

which is a generalization of the familiar formula

$g^2 = \bar{\alpha}_P - \alpha_1$ [see the sentence after Eq. (4.13) for the case of the leading-trajectory approximation]. (ii) The two equal-spacing rules (2.20) and (2.22) $\alpha_2 = \frac{1}{2}(\alpha_1 + \alpha_3)$, $\alpha_4 = \frac{1}{2}(\alpha_1 + \alpha_5)$, and also the relation $\alpha_5 = \frac{1}{2}(\alpha_3 + \alpha_6)$ are valid. These equal-spacing rules and the relation (4.24) can be shown to follow from bootstrap in the Reggeon sector for case (b) by studying the set of equations in which all the trajectories are included in the unitarity sum.

With the above two assumptions holding, the case in which all dual diagrams are taken into account

TABLE I. Comparison of dual unitary scheme with data for cross-section ratios.

F_λ, F_C	$F_\lambda=1, F_C=1$			$F_\lambda=0.9, F_C=0.8$			$F_\lambda=0.8, F_C=0.7$			Empirical values
	-2	-4	-6	-2	-4	-6	-2	-4	-6	
$\alpha_6(0)$										(0.8) ^a
$R_2=R_{K^*}$	0.75	0.75	0.75	0.64	0.64	0.64	0.55	0.55	0.55	(0.73±0.1) ^b
$R_3=R_\phi$	0.50	0.50	0.50	0.35	0.35	0.35	0.23	0.23	0.23	0.45±0.2 ^{c,g}
$R_4=R_{D^*}$	0.58	0.55	0.54	0.45	0.43	0.42	0.39	0.37	0.37	(~0.52) ^d
$R_5=R_{F^*}$	0.33	0.30	0.29	0.20	0.18	0.17	0.13	0.12	0.12	~(0.23±0.08) ^e
$R_6=R_\psi$	0.17	0.10	0.07	0.08	0.05	0.04	0.06	0.03	0.02	~0.04 ^{f,g}

$g^2=\gamma_{11}=g_{\rho\rho f}^2=0.5$

^aIn the absence of data for K^*p , we quote the experimental ratio for $\sigma(Kp)/\sigma(\pi p)$. For detailed comparison with the CGZ model see Ref. 15.

^bThe value obtained from the quark-model relation (5.50) together with $R_3^{\text{exp}}=0.45\pm 0.2$.

^cAs quoted in Ref. 6 or Ref. 16.

^dThe value obtained from Eq. (5.51) together with $R_6^{\text{exp}}\sim 0.04$.

^eThe value obtained from Eq. (5.52) together with $R_6^{\text{exp}}\sim 0.04$.

^fThe experimental values from photoproduction $\sigma(\rho p)\simeq 23$ mb (Ref. 16) and $\sigma(\psi N)\simeq 1$ mb (Ref. 17) have been used. Note, however, that for the latter, especially, the off-mass-shell problem of the vector-dominance model is not completely understood.

^gSee also V. Barger, lectures delivered at McGill Inst. of Particle Physics, 1975 (unpublished).

coincides with the case when only one leading diagram is kept in the unitarity sum. The difference is only in the coupling constant g^2 .

V. THE SLOPE PARAMETER OF DIFFERENTIAL CROSS SECTION FOR DIFFRACTIVE SCATTERING

We denote by $2b(s)$ the slope of the diffraction peak for large s defined as

$$2b(s) = \left(\frac{\partial}{\partial t} \ln \frac{d\sigma}{dt} \right)_{t=0} \quad (5.1)$$

and consider the predictions of the dual unitary scheme for this parameter. While with respect to the total-cross-section ratios the predictions of the dual unitarization model coincide with those of the CGZ model, as shown below, the predictions of the two models for the slope parameters differ.

We proceed in a similar way as Carlitz, Green, and Zee⁶ and assume s -channel helicity conservation for the differential cross section

$$\frac{d\sigma}{dt} = |F_{\text{nonflip}}|^2 + |F_{\text{flip}}|^2$$

TABLE II. Comparison of dual unitarization and CGZ models for diffractive slopes in GeV^{-2} .

$\alpha_\psi(0)$	Dual unitarization						CGZ model						Experiment
	$\alpha'_p=0.4 \text{ GeV}^{-2}$			$\alpha'_p=0.2 \text{ GeV}^{-2}$			$\alpha'_p=0.4 \text{ GeV}^{-2}$			$\alpha'_p=0.2 \text{ GeV}^{-2}$			
	-2	-4	-6	-2	-4	-6	-2	-4	-6	-2	-4	-6	
$b(K^*N) - b(\rho N)$	-0.27	-0.27	-0.27	-0.30	-0.30	-0.30	-0.20	-0.20	-0.20	-0.27	-0.27	-0.27	(-0.32±0.15) ^a
$b(\phi N) - b(\rho N)$	-0.80	-0.80	-0.80	-0.90	-0.90	-0.90	-0.60	-0.60	-0.60	-0.80	-0.80	-0.80	-0.95±0.45 ^b
$b(D^*N) - b(\rho N)$	-0.19	-0.12	-0.09	-0.21	-0.14	-0.10	-0.14	-0.09	-0.07	-0.19	-0.12	-0.09	~(-0.11) ^c
$b(F^*N) - b(\rho N)$	-0.93	-0.89	-0.87	-1.04	-1.00	-0.98	-0.69	-0.66	-0.65	-0.93	-0.89	-0.87	~(-1.0) ^d
$b(\psi N) - b(\rho N)$	-1.30	-1.34	-1.37	-1.46	-1.52	-1.55	-0.96	-0.98	-0.99	-1.30	-1.34	-1.37	-1.80 ^e -1.25 ^f

^aThe value predicted from (6.3) and (6.4) together with the experimental value $b(\phi N) - b(\rho N) = -0.95 \pm 0.45 \text{ GeV}^{-2}$.

^bFrom $2b(\rho N) = 6.5 \pm 0.2 \text{ GeV}^{-2}$ (Ref. 16) and $2b(\phi N) = 4.6 \pm 0.70$ (Ref. 16).

^cThe value obtained from (6.5) and (6.7) together with experimental value $b(\psi N) - b(\rho N) \sim -1.25 \text{ GeV}^{-2}$ (Knapp *et al.*, Ref. 17).

^dThe value obtained from (6.6), (6.4), and (6.7) together with experimental value $b(\phi N) - b(\rho N) = -0.95 \pm 0.45 \text{ GeV}^{-2}$ and $b(\psi N) - b(\rho N) \sim -1.25 \text{ GeV}^{-2}$ and $\alpha_\psi(0) = -4$.

^eFrom $2b(\psi N) \sim 2.9 \text{ GeV}^{-2}$ (Camerini *et al.*, Ref. 17).

^fFrom the value $2b(\psi N) \sim 4.0 \text{ GeV}^{-2}$ (Knapp *et al.*, Ref. 17).

of elastic scattering and neglect the real part of F_{nonflip} in calculating the diffraction slope b . Then we have

$$b_i - b_j = \left(\frac{\partial}{\partial t} \ln \frac{\beta_i^P}{\beta_j^P} \right)_{t=0}. \quad (5.2)$$

We take the ratios of the Pomeron residues β_i^P/β_j^P from the formulas (4.14)–(4.19). Further, we envisage the possibility that the t dependence of β_i^P/β_j^P is introduced by giving corresponding t dependence to $\alpha_i(0)$ and $\alpha_P(0)$. Then we can derive the following relations:

$$b(K^*N) - b(\rho N) = r'_1(0)/[1 + r_1(0)], \quad (5.3)$$

$$b(\phi N) - b(\rho N) = r'_1(0)/r_1(0), \quad (5.4)$$

$$\begin{aligned} r_1(0)_{\text{DUS}} &= \frac{\bar{\alpha}_P(0) - \alpha_1(0)}{\bar{\alpha}_P(0) - \alpha_3(0)}, & r_1(0)_{\text{CGZ}} &= \frac{\alpha_P(0) - \alpha_f(0)}{\alpha_P(0) - \alpha_{f'}(0)}, \\ r'_1(0)_{\text{DUS}} &= \frac{[\alpha'_P/2 - \alpha'_1(0)][\bar{\alpha}_P(0) - \alpha_3(0)] - (\alpha'_P/2 - \alpha'_3)[\bar{\alpha}_P(0) - \alpha_1(0)]}{[\bar{\alpha}_P(0) - \alpha_3(0)]^2}, \\ r'_1(0)_{\text{CGZ}} &= \frac{(\alpha'_P - \alpha'_f)[\alpha_P(0) - \alpha_{f'}(0)] - (\alpha'_P - \alpha'_{f'})[\alpha_P(0) - \alpha_f(0)]}{[\alpha_P(0) - \alpha_{f'}(0)]^2}, \\ r_2(0)_{\text{DUS}} &= \frac{\bar{\alpha}_P(0) - \alpha_1(0)}{\bar{\alpha}_P(0) - \alpha_6(0)}, & r_2(0)_{\text{CGZ}} &= \frac{\alpha_P(0) - \alpha_f(0)}{\alpha_P(0) - \alpha_{f_C}(0)}, \\ r'_2(0)_{\text{DUS}} &= r'_1(0)_{\text{DUS}} \Big|_{\text{replace } \alpha_3 \rightarrow \alpha_6}, & r'_2(0)_{\text{CGZ}} &= r'_1(0)_{\text{CGZ}} \Big|_{\text{replace } \alpha_{f'} \rightarrow \alpha_{f_C}}, \end{aligned} \quad (5.8)$$

where

$$\bar{\alpha}_P(0) = [1 + \alpha_P(0)]/2,$$

and the prime denotes a derivative with respect to t .

As an illustration, we choose the following representative forms¹⁴ for the Regge and Pomeron trajectories:

$$\begin{aligned} \alpha_{\omega-f} &= \alpha_{\rho-A_2}(t) \equiv \alpha_1(t) = 0.5 + 0.90t, \\ \alpha_{\phi-f'} &\equiv \alpha_3(t) = 0 + 0.80t, \\ \alpha_{\psi-f_C} &\equiv \alpha_6(t) = -2 + 0.5t, \quad -4 + 0.5t, \quad -6 + 0.5t, \end{aligned}$$

and

$$\alpha_P(t) = 1 + 0.4t, \quad 1 + 0.2t.$$

$$b(D^*N) - b(\rho N) = r'_2(0)/[1 + r_2(0)], \quad (5.5)$$

$$b(F^*N) - b(\rho N) = [r'_1(0) + r'_2(0)]/[r_1(0) + r_2(0)] \quad (5.6)$$

$$b(\psi N) - b(\rho N) = r'_2(0)/r_2(0), \quad (5.7)$$

where

$$r'_i(0) = \left. \frac{d}{dt} r_i(t) \right|_{t=0}, \quad i = 1, 2.$$

Let us list the expressions for the $r_i(0)_{\text{DUS}}, r'_i(0)_{\text{DUS}}$ of the dual unitarization scheme obtained from Eqs. (4.19) and for the f -dominated Pomeron model of CGZ,⁶ $r_i(0)_{\text{CGZ}}, r'_i(0)_{\text{CGZ}}$ obtained from (4.21):

The estimated values for $b(VN) - b(\rho N)$ obtained in our and in the CGZ models for two different values $\alpha'_P = 0.4$ and 0.2 and for three values $\alpha_\psi(0) = -2, -4, \text{ and } -6$ are summarized in Table II.

ACKNOWLEDGMENTS

We are very grateful to M. Bishari for many fruitful discussions, for constructive criticism, and contributions. We thank A. J. Buras, P. Hoyer, N. Törnqvist, and Y. Zarmi for useful discussions, and Kazuo Katsuura for help in numerical evaluations. One of us (M.H.) would like to thank the Research Institute for Theoretical Physics, Helsinki, for their hospitality.

¹G. Veneziano, Phys. Lett. **43B**, 413 (1973); see also Nucl. Phys. **B74**, 365 (1974); Phys. Lett. **52B**, 220 (1974).

²Huan Lee, Phys. Rev. Lett. **30**, 719 (1973).

³H. M. Chan and J. E. Paton, Phys. Lett. **46B**, 228 (1973); H. M. Chan, J. E. Paton, and S. T. Tsou, Nucl. Phys. **B86**, 479 (1975); H. M. Chan, J. E. Paton, S. T. Tsou,

and S. W. Ng, Nucl. Phys. **B86**, 479 (1975); G. F. Chew and C. Rosenzweig, Phys. Lett. **58B**, 93 (1975); Phys. Rev. D **12**, 3907 (1975); N. Sakai, Nucl. Phys. **B99**, 167 (1975); M. Bishari, Phys. Lett. **59B**, 416 (1975); G. F. Chew and C. Rosenzweig, Nucl. Phys. **B104**, 290 (1976); G. Veneziano, *ibid.* **B108**, 285 (1976); C. Schmid, D. M. Webber, and C. Sorensen, *ibid.* **B111**, 317 (1976);

- H. M. Chan, J. Kwiecinski, and R. G. Roberts, *Phys. Lett.* **60B**, 367 (1976); M. Fukugita, T. Inami, N. Sakai, and S. Yazaki, *Nucl. Phys.* **B121**, 93 (1977); Y. Eylon, *ibid.* **B118**, 95 (1977); **B118**, 117 (1977); T. Inami, K. Kawarabayashi, and S. Kitakado, *Phys. Lett.* **72B**, 127 (1977); S. T. Tsou, *Phys. Rev. D* **16**, 2353 (1977).
- ⁴C. Schmid and C. Sorensen, *Nucl. Phys.* **B96**, 209 (1975); N. Papadopoulos, C. Schmid, C. Sorensen, and D. M. Webber, *ibid.* **B101** 189 (1975).
- ⁵G. F. Chew, C. Rosenzweig, and P. R. Stevens, *Nucl. Phys.* **B110**, 355 (1976).
- ⁶R. Carlitz, M. B. Green, and A. Zee, *Phys. Rev. Lett.* **26**, 1515 (1971); *Phys. Rev. D* **4**, 3439 (1971).
- ⁷P. G. O. Freund and R. J. Rivers, *Phys. Lett.* **29B**, 510 (1969).

⁸This can be most easily seen in another equivalent way, namely, by writing, instead of (2.10)–(2.16), an integral equation for the total amplitude $A = A_P + A_f$, in which f never arises.

⁹We have neglected the cross terms between α_1 and α_2 exchanges. In the Reggeon sector, because of the phase factor

$$\frac{1}{2}(e^{-i\pi\alpha_1}e^{i\pi\alpha_2} + e^{-i\pi\alpha_2}e^{i\pi\alpha_1}) = \cos \pi(\alpha_1 - \alpha_2),$$

the contribution of the cross terms vanishes, but only if $\alpha_1 - \alpha_2 = \frac{1}{2} + n$. In the Pomeron sector, however, the contribution of the cross terms with twisted Reggeon propagators in general does not vanish unless such exchanges are forbidden by considerations such as isospin and G parity.

¹⁰It would be interesting to study the consistency of bootstrap in the Reggeon sector and to find its solution within the general model (i.e., without the duality-diagrams constraints) discussed here. It may well come out that the only consistent solution is the one dictated by duality diagrams. It is also interesting to notice that a relation of the kind $\gamma_{11}\gamma_{22} = \gamma_{12}^2$, which is the consequence of semilocal duality, does not hold within the formal model discussed here.

¹¹D. Amati, M. LeBellac, G. M. Marchesini, and M. Ciafaloni, *Nucl. Phys.* **B112**, 107 (1976).

¹²A. Capella, J. Kaplan, and J. Tran Thanh Van, *Nucl. Phys.* **B97**, 493 (1975).

¹³However, this comparison is not to be taken literally, since in Ref. 12 there is a single leading pole at $\alpha_P = 1 + \epsilon$ with $\epsilon \approx 0.13$, while from (3.12) one has two poles at $\alpha_1^P = 1 + \epsilon$ and $\alpha_2^P = 1 - \epsilon$. Condition $\epsilon^2 \geq 8\gamma_{12}^2$ can be derived from Eqs. (3.7)–(3.12) and with a certain choice for the coupling constants γ_{ij} and the intercepts α_i , the second pole at $1 - \epsilon$ can have a positive residue.

¹⁴T. Inami, *Phys. Lett.* **56B**, 291 (1975).

¹⁵R. G. Roberts, *Nucl. Phys.* **B116**, 334 (1976).

¹⁶J. Ballam *et al.*, *Phys. Rev. D* **7**, 3150 (1973).

¹⁷B. Knapp *et al.*, *Phys. Rev. Lett.* **34**, 1040 (1975); U. Camerini *et al.*, *ibid.* **35**, 483 (1975); also W. Y. Lee, in *Proceedings of the 1975 International Symposium on Lepton and Photon Interactions at High Energies*, Stanford, California, edited by W. T. Kirk (SLAC, Stanford, 1976), p. 213.